Diagn Interv Radiol 2022; 28:5–11

ABDOMINAL IMAGING

ORIGINAL ARTICLE

Fat- and iron-corrected ADC to assess liver fibrosis in patients with chronic hepatitis B

Zhongxian Pan*
Zhujing Li*
Fanqi Meng
Yuanming Hu
Xiaoyong Zhang
Yueyao Chen

PURPOSE

We aimed to evaluate the diagnostic performance of apparent diffusion coefficient (ADC) in assessing liver fibrosis after correcting for the effects of hepatic steatosis or iron deposition.

METHODS

Seventy-three patients with chronic hepatitis B (CHB) were included in this retrospective study. The aspartate aminotransferase-to-platelet ratio index (APRI) was calculated for classification of the fibrosis grade. Significant fibrosis and cirrhosis were diagnosed with the APRI. The proton density fat fraction (PDFF), R2*, and ADC values were measured. The impact of the PDFF and R2* on the ADC was analyzed. The PDFF- and R2*-corrected ADC values (ADC_{PDFF} and ADC_{R2*}) were calculated according to linear regression equations. The diagnostic performance of uncorrected ADC (ADC_u), ADC_{PDFF} and ADC_{R2*} in predicting significant fibrosis and cirrhosis was assessed, and the area under the curve (AUC) values were compared.

RESULTS

Among the 73 patients in this study, the mean ADC was 0.866 ± 0.084×10^{-3} mm^2/s, the mean R2* was 60.24 (42.77, 85.37) 1/s, and the mean PDFF was 2.90% (1.60%- 4.80%). The ADC was negatively correlated with the PDFF (r= -0.298, P = .010) and R2* (r = -0.457, P < .001). Linear regression analysis showed that the PDFF and R2* were independent factors of the ADC (β= -0.315, P = .007, R^2= 0.099 and β= -0.493, P < .001, R^2= 0.243, respectively). Compared with the uncorrected ADC (r= -0.307, P = .022), the correlation between the ADC_{PDFF} and fibrosis grade increased (r= -0.513, P < .001), and the correlation between the ADC_{R2*} and fibrosis grade decreased (r=-0.168, P = .215). The AUC of the ADC_{PDFF} was significantly larger than that of the ADC_u in the diagnosis of significant fibrosis and cirrhosis, which increased from 0.68 to 0.81 (P = .003) for predicting significant fibrosis and from 0.75 to 0.84 (P = .009) for predicting cirrhosis. The AUCs for the ADC_{R2*} in the diagnosis of significant fibrosis and cirrhosis were both lower than that for the uncorrected ADC (P = .206 and P = .109, respectively).

CONCLUSION

After correcting for the effects of steatosis, the diagnostic performance of the ADC for significant fibrosis and cirrhosis increased. The ADC corrected for the effects of steatosis may be more reliable for identifying liver fibrosis.

From the Department of Radiology (Z.P., Z.L., F.M., Y.H., Y.C. ✉ *rchenyueyao@163.com*), Shenzhen Traditional Chinese Medicine Hospital (The Fourth Clinical Medical College of Guangzhou University of Chinese Medicine), Shenzhen, China; MR Collaborations (X.Z.), Siemens Healthcare Ltd., Shenzhen, China.

*Zhongxian Pan and Zhujing Li contributed equally to this work.

Received 5 May 2021; revision requested 30 May 2021; last revision received 31 July 2021; accepted 1 September 2021.

Published online 19 November 2021.

DOI 10.5152/dir.2021.21471

Fibrosis staging is an essential step in the clinical management of patients with chronic hepatitis B (CHB) infection to identify those requiring treatment or screening for portal hypertension and hepatocellular carcinoma. Liver biopsy is currently the gold standard for the diagnosis of hepatic fibrosis. However, biopsy is invasive, semiquantitative, observer dependent, and prone to sampling variability.[1] Furthermore, repeated biopsy for the purpose of monitoring disease progression is not the best option and has poor patient acceptance.

Therefore, alternative noninvasive approaches have been developed to assess liver fibrosis, including routine biochemical and hematological tests, serum markers of connective tissue, quantitative imaging and scoring systems using a combination of clinical and/or laboratory tests.[2-4] In international guidelines, the aspartate aminotransferase to platelet ratio index (APRI) is recommended as a noninvasive tool to detect liver cirrhosis and significant fibrosis in resource-limited settings.[5]

You may cite this article as: Pan Z, Li Z, Meng F, Hu Y, Zhang X, Chen Y. Fat- and iron-corrected ADC to assess liver fibrosis in patients with chronic hepatitis B. *Diagn Interv Radiol*. 2022;28(1):5-11.

Recent studies have also examined the usefulness of diffusion-weighted magnetic resonance imaging (DWI) for the diagnosis and staging of fibrosis. The complex assembly of collagen fibers, glycosaminoglycans, and proteoglycans that constitute liver fibrosis may restrict molecular diffusion measured by DWI, which reduces the apparent diffusion coefficient (ADC).[6] Several investigators have successfully used DWI to assess hepatic fibrosis and cirrhosis,[6,7] but results vary, probably because of the effects of hepatic steatosis and iron overload. Biopsy-validated studies have confirmed that the ADC is affected by liver steatosis and iron overload,[8,9] and hepatic steatosis and iron overload are prevalent during the course of CHB.[10]

Therefore, correcting for the effects of hepatic steatosis and iron deposition on ADC values may be helpful for studying the clinical value of the ADC in assessing hepatic fibrosis. A few studies have explored correcting the effect of fat on the ADC, but most of these studies are based on magnetic resonance imaging (MRI),[11,12] the principle of which is complicated and difficult to repeat directly. Several other studies used regression equations to correct quantitative values;[10,13] they first evaluated the influence value of X on Y and then subtracted the influence value from Y to correct for influence. This method is simpler and easier to implement.

To our knowledge, the diagnostic performance of the ADC after correcting for the effects of hepatic steatosis or iron deposition in liver fibrosis staging has not been thoroughly studied. Therefore, the purpose of our study was to explore the effects of liver steatosis and iron overload on the ADC and to correct for them using a regression equation. Furthermore, we evaluated the diagnostic performance of the corrected ADC in liver fibrosis staging.

Main points

- Fat and iron deposition affect ADC values in patients with chronic hepatitis B.
- The ADC decreases with increasing fat and iron contents.
- The effects of fat and iron should be noted when evaluating liver fibrosis using the ADC.
- The ADC corrected for the effects of steatosis may be more reliable for diagnosing liver fibrosis.

Methods

Patients

This retrospective study was approved by our institutional review board (K2019-070-01), and the requirement for written informed consent was waived. Sample size estimation was performed based on the results of Fujimoto et al.[7] Between October 2018 and March 2019, 85 patients clinically diagnosed with CHB underwent liver MRI examination at our hospital. Twelve patients were excluded for meeting the following exclusion criteria: water-fat swapping in the Dixon sequence (n=9), resulting in an abnormally high proton density fat fraction (PDFF) (>90%); liver tumors larger than 20 mm in diameter (n=2); and a history of liver surgery (n=1). Finally, 73 patients were included, with 61 males and 12 females. These patients had no history of hereditary hemochromatosis or repeated blood transfusions and no other etiologic causes, such as hepatitis C virus infection or alcoholic hepatitis.

Liver fibrosis grading by APRI

Fifty-six of the 73 patients underwent liver function tests and routine blood tests within 2 weeks before or after the MRI exam. Aspartate aminotransferase (AST), alanine aminotransferase (ALT) and the platelet count (PLT) were recorded. On the basis of these biological parameters, the following noninvasive fibrosis score was calculated: *aspartate aminotransferase–to-platelet ratio index (APRI)= [(aspartate aminotransferase/upper limit of normal aspartate aminotransferase) × 100]/platelet count (10^9/L)*. In the 2015 World Health Organization (WHO) guidelines on CHB management, the APRI was recommended as a noninvasive tool to detect significant liver fibrosis and cirrhosis in resource-limited settings.[5] A meta-analysis of 64 studies showed that the area under the curve (AUC) values of the APRI for significant fibrosis (≥F2) and cirrhosis (F4) were both 0.76.[14] Cutoff APRI values of 0.5 and 1 had acceptable diagnostic performance.[2,4,15] Therefore, in this study, fibrosis grade was evaluated using APRI scores: grade 1, APRI< 0.5; grade 2, 0.5≤ APRI< 1; and grade 3, APRI≥ 1.

MRI technique

A 3T MRI scanner (MAGNETOM, Prisma, Siemens Healthcare) with a 16-channel body phased-array coil was used. Each patient fasted for more than 4 hours and then assumed a comfortable supine position. All sequences were acquired in a transverse orientation. In addition to routine clinical sequences, the following sequences were included: 1) three-dimensional (3D) multiecho Dixon: repetition time (TR)= 9 ms, echo time (TE)= 1.1/2.46/3.69/4.92/6.15/7.38 ms, field of view (FOV)= 380×380 mm^2, slice thickness= 3.5 mm, average= 1, and flip angle= 4°. R2* and PDFF maps were automatically calculated at the end of each acquisition. The acquisition time was 11 s. 2) DWI: TR= 6700 ms, TE= 46 ms, FOV= 380×380 mm^2, slice thickness= 5 mm, *b* value= 50/1000 s/mm^2. The spin echo single-shot echo-planar imaging (SE-SS-EPI) technique was used. Spectral presaturation attenuated inversion recovery (SPAIR) technology was used for fat suppression. To investigate the diagnostic performance of the ADC in liver fibrosis staging, *b* values of 50 and 1000 s/mm^2 were used in this study, as suggested by Fujimoto et al.[7] and Bulow et al.[9] T2* shortening due to iron deposition is much stronger at 3T and high *b* values and will thus reduce the signal-to-noise ratio (SNR) of DWI. Therefore, to ensure image quality, technologies such as 4-Scan Trace and monopoplar sequences were used to reduce the TE (46 ms) in this study. ADC maps were automatically calculated at the end of each acquisition with the following equation: $Si= S0* e(-bi*ADC)$, where S_i is the signal intensity (SI) at a *b* value of 1000 and S_0 represents the estimated SI at a *b* value of 50.

Image analysis

Image analysis was performed with a Siemens Syngo via workstation by an author (P.Z.X.) with 8 years of experience in liver MRI who was blinded to the clinical data.

PDFF values were measured by manually placing circular regions of interest (ROIs) of at least 10 mm in diameter in each of the nine Couinaud liver segments on PDFF maps, carefully avoiding the liver edge, areas of motion artifacts, and visible blood vessels and bile ducts.[16] Hines et al.[17] suggested that multiple regions of interest averaged across the liver improved the precision of PDFF estimation. R2*, goodness of fit and ADC values were measured on R2* maps, goodness of fit maps and ADC maps, respectively, and ROIs were positioned in accordance with the positioning used for the PDFF maps. The mean PDFF, R2*, goodness of fit and ADC values averaged across all nine ROIs were recorded; only the mean values across the nine ROIs were consid-

ered in this study. To ensure data accuracy for PDFF and R2* measurements, patients with water-fat swapping or goodness of fit >5% in the Dixon sequence were excluded. Water-fat swapping caused an abnormally high PDFF (18), and goodness of fit >5% suggested unreliable fitting calculation (19). A PDFF ≥5.04% was defined as steatosis, and R2* ≥58.7 1/s was diagnosed as hepatic iron overload.[20]

ADC correction

Referring to the correction method of Karlsson et al.,[10] linear regression analysis was performed to build a linear regression equation between the ADC and PDFF: $ADC = a + b \times PDFF$, where a is the constant and b is the regression coefficient. The following equation was used to correct for the effect of the PDFF on the ADC: $ADC_{PDFF} = ADC - b \times PDFF$. A similar method was used to calculate the R2*-corrected ADC (ADC_{R2*}).

Statistical analysis

Correlation between the uncorrected ADC (ADC_u) and potential variables (age, sex, R2*, PDFF and fibrosis grade) were assessed using Spearman rank correlation coefficients. Linear regression analysis was performed to identify independent factors of the ADC. The ADC corrected for the effects of liver steatosis or iron deposition was calculated according to a linear regression equation. Differences between fibrosis grades for continuous variables were compared using one-way analysis of variance (normal distribution) or Kruskal-Wallis test (non-normal distribution). The correlation between the corrected ADC and hepatic fibrosis grade was evaluated and compared with that of the uncorrected ADC. The diagnostic performance of the ADC_u, ADC_{PDFF} and ADC_{R2*} in predicting significant fibrosis and cirrhosis was assessed, and the AUC values were compared using DeLong test. Sensitivity, specificity, and positive and negative predictive values for the classification of significant fibrosis and cirrhosis were calculated with standard formulas according to the values of these indexes. Optimal cut-off values were selected using a common optimization step that maximized the Youden index, and sensitivity and specificity were computed from the same data without further adjustment.

Normally distributed continuous variables were given in means and standard deviations (SD), and non-normally distributed continuous variables were represented in medians and first quartile (Q1)- third quartile(Q3). Categorical variables were presented as numbers and percentages. Statistical analyses were performed using SPSS (version 17, SPSS) and SigmaPlot (version 14.0, SigmaPlot Software). The level for statistical significance was set to $P < .05$.

Results

A total of 73 patients with CHB were included; the clinical characteristics of the cohort are shown in Table 1. Table 2 shows the data for different fibrosis grades. With increasing liver fibrosis grades, the PDFF tended to decrease, and the PDFF of fibrosis grade 1 was significantly higher than that of grade 3 ($P = .023$). The goodness of fit of the multiecho Dixon sequence was 1.62 (1.20-2.10) in this study, which was acceptable for the evaluation of R2* and the PDFF. Figure 1 shows that the ADC was slightly reduced in patients with steatosis and significantly reduced in patients with iron overload and steatosis plus iron overload compared with patients without steatosis and iron overload.

The ADC was negatively correlated with the PDFF (r= -0.298, $P = .010$) (Figure 2a) and R2* (r = -0.457, $P < .001$) (Figure 2b). Linear regression analysis showed that the PDFF and R2* were independent factors of the ADC (β= -0.315, $P = .007$, R^2= 0.099 and β= -0.493, $P < .001$, R^2= 0.243, respectively) and provided the following regression: ADC= 899.612- 8.865× PDFF, ADC= 915.057- 0.622× R2*. The unit of the ADC is 10^{-6} mm^2/s.

These results indicate that the ADC decreases by close to 8.865× PDFF (10^{-6} mm^2/s) for every patient. Referring to the correction method of Karlsson et al.,[10] this model was used to create a PDFF-corrected ADC (ADC_{PDFF}) by adding 8.865× PDFF for each

Table 1. Characteristics of the 73 patients

	Mean ± SD/ Median (Q1-Q3)
Age (years)	50 (41.5-58.5)
Gender (male/female), n	61/12
Serum laboratory values	
Aspartate aminotransferase (U/L)	29.15 (21.65- 46.58)
Alanine aminotransferase (U/L)	26.30 (19.00- 37.90)
Platelet count (10^9/L)	147.96 ± 66.65
APRI	0.53 (0.31-1.18)
Imaging	
ADC ($10^{-3}mm^2/s$)	0.866 ± 0.084
R2* (1/s)	60.24 (42.77-85.37)
PDFF (%)	2.90 (1.60-4.80)

SD, standard deviation; Q1, first quartile; Q3, third quartile; APRI, aspartate aminotransferase–to-platelet ratio index; ADC, apparent diffusion coefficient; PDFF, proton density fat fraction.

Table 2. Data for different fibrosis grades

Fibrosis grade	n (%)	APRI	PDFF (%)	R2* (1/s)	ADC_u ($10^{-3}mm^2/s$)	ADC_{PDFF} ($10^{-3}mm^2/s$)	ADC_{R2*} ($10^{-3}mm^2/s$)
1	26 (46.43)	0.31 (0.25-0.36)	4.10 (2.45-5.78)	61.50 (42.75-78.50)	0.883 ± 0.070	0.925 ± 0.065	0.925±0.057
2	12 (21.43)	0.62 (0.54-0.72)	2.16 (1.11-7.85)	78.00 (48.88-88.25)	0.856 ± 0.085	0.891±0.054	0.905±0.066
3	18 (32.14)	1.88 (1.18-3.50)	2.41 (1.34-3.00)	78.03 (42.46-158.00)	0.808 ± 0.082	0.832±0.078	0.883±0.086

APRI, aspartate aminotransferase–to-platelet ratio index; PDFF, proton density fat fraction; ADC, apparent diffusion coefficient ; ADC_u, uncorrected ADC; ADC_{PDFF}, PDFF-corrected ADC; ADC_{R2*}, R2*-corrected ADC.

Table 3. Comparison of the diagnostic performance of the ADC_u, ADC_{PDFF}, and ADC_{R2*} for significant fibrosis (≥F2) and cirrhosis (F4)

		AUC (95% CI)	Cutoff value	Sensitivity (95% CI)	Specificity (95% CI)	*P*	
≥F2	ADC_{PDFF}	0.81 (0.69-0.93)	0.908	0.83 (0.69-0.92)	0.73 (0.52-0.88)	< 0.001	
	ADC_u	0.68 (0.53-0.82)	0.903	0.93 (0.83-0.99)	0.42 (0.23-0.63)	0.023	0.003
	ADC_{R2*}	0.62 (0.47-0.77)	0.873	0.40 (0.26-0.56)	0.85 (0.65-0.96)	0.123	0.206
F4	ADC_{PDFF}	0.84(0.73-0.94)	0.879	0.78 (0.60-0.90)	0.82 (0.66-0.92)	< 0.001	
	ADC_u	0.75 (0.62-0.88)	0.843	0.72 (0.54-0.85)	0.79 (0.63-0.91)	0.002	0.009
	ADC_{R2*}	0.65 (0.49-0.82)	0.897	0.67 (0.48-0.81)	0.68 (0.51-0.83)	0.068	0.109

ADC, apparent diffusion coefficient; PDFF, proton density fat fraction; AUC, area under the curve; CI, confidence interval; ADC_u, uncorrected ADC; ADC_{PDF}F, PDFF-corrected ADC; ADC_{R2*}, R2*-corrected ADC.

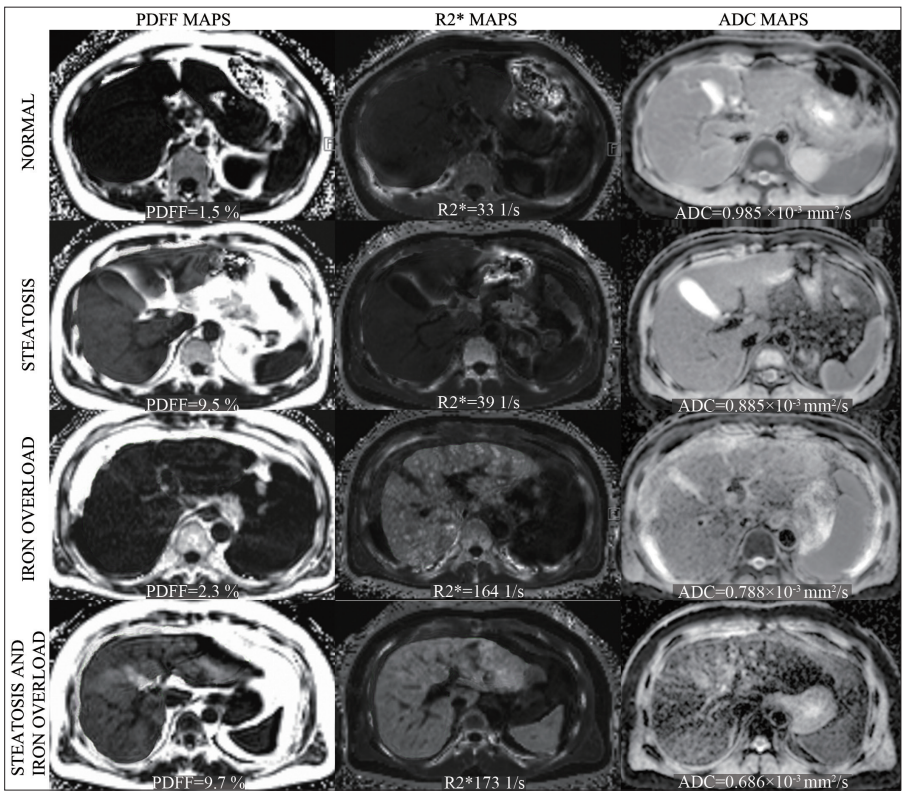

Figure 1. Examples of a normal liver vs. livers with steatosis, iron overload, and steatosis plus iron overload. A PDFF ≥5.04% was defined as steatosis, and R2* ≥58.7 1/s was diagnosed as hepatic iron overload. The ADC was slightly reduced in patients with steatosis and significantly reduced in patients with iron overload and steatosis plus iron overload compared with that in patients without steatosis and iron overload.

patient: $ADC_{PDFF} = ADC + 8.865 \times PDFF$. In addition, the ADC value decreased by close to 0.622× R2* (10^{-6} mm^2/s) for every patient. This model was used to create an R2*-corrected ADC (ADC_{R2*}) by adding 0.622× R2* for each patient: $ADC_{R2*} = ADC + 0.622 \times R2*$.

The ADC_u was negatively correlated with fibrosis grade (r= -0.307, *P* = .022) (Figure 3a). Compared with ADC_u, the correlation between the ADC_{PDFF} and fibrosis grade increased from r= -0.307 to r= -0.513 (*P* < .001) (Figure 3b), and the correlation between the ADC_{R2*} and fibrosis grade decreased to r= -0.168 (*P* = .215) (Figure 3c). The PDFF of fibrosis grade 1 was significantly higher than that of grade 3 (*P* = .023). Figure 4 shows that with increasing liver fibrosis grading, the ADC tended to increase. The ADC_u was significantly different only between fibrosis grades 1 and 3 (*P* = .003). However, the ADC_{PDFF} was statistically different not only between fibrosis grades 1 and 3 (*P* < .001) but also between grades 2 and 3 (*P* = .022).

The diagnostic performance of the ADC_u, ADC_{PDFF} and ADC_{R2*} in predicting significant fibrosis and cirrhosis is shown in Table 3 and Figure 5. The AUC for the ADC_{PDFF} was significantly larger than that for the ADC_u in assessing significant fibrosis and cirrhosis, which increased from 0.68 to 0.81 (*P* = .003) for significant fibrosis prediction and from 0.75 to 0.84 (*P* = .009) for cirrhosis prediction. The AUC values for the ADC_{R2*} in predicting significant fibrosis and cirrhosis were 0.62 and 0.65, respectively, which were less than those for the ADC_u (*P* = .206 and *P* = .109, respectively).

Discussion

The effects of hepatic steatosis and iron deposition on ADC values have caused concern. Our purpose was to explore the effect of liver steatosis and iron overload on the ADC and to evaluate the diagnostic performance of the corrected ADC for liver fibrosis staging. Our study suggested that both the PDFF and R2* were correlated with the ADC and were independent factors of the ADC. Compared with the uncorrected ADC, the correlation between the ADC_{PDFF} and fibrosis grade increased, while the correlation between the ADC_{R2*} and fibrosis grade decreased. The AUC for the ADC_{PDFF} was significantly larger than that of the ADC_u in the diagnosis of significant fibrosis and cirrhosis. The AUC values for the ADC_{R2*} in the diagnosis of significant fibrosis and cirrhosis were both less than those for the uncorrected ADC.

Previous studies have explored the performance of the ADC in diagnosing liver fibrosis. Similar to most previous studies,[7,21] our findings showed that liver fibrosis grade was significantly negatively correlated with ADC values. The complex assembly of collagen fibers, glycosaminoglycans, and proteoglycans that constitutes liver fibrosis may restrict molecular diffusion, which reduces the ADC. Previous studies showed excellent performance of the ADC for the detection

of hepatic fibrosis, with AUC ranges of 0.69-0.93 for significant fibrosis and 0.79-0.92 for cirrhosis.[6,7,22,23] However, in these studies, the AUC and cutoff values varied considerably. Even in studies with similar DWI protocols, the ADC values were quite different.[7, 23] Therefore, in addition to imaging technology factors, these differences might also be related to other influencing factors of the ADC, such as liver steatosis and iron overload. Unlike hereditary hemochromatosis and repeated blood transfusions, hepatic iron overload in patients with chronic liver disease is often mild.[24, 25] The R2* of CHB patients in this study was 60.24 (42.77-85.37) 1/s, and the PDFF was 2.90% (1.60%-4.80%), which are consistent with the results of a study of 691 patients with CHB.[26]

Our study showed a negative correlation between ADC and PDFF values and suggested that ADC values were affected by fatty liver. First, incomplete fat suppression was believed to be one of the main reasons. The frequency of two of the fat peaks (5.3 ppm for olefinic acid and 4.2 ppm for glycerol) is very close to that of the water peak (4.7 ppm). These lipid peaks cannot be thoroughly suppressed without inhibiting the water peak at the same time. Therefore, this residual fat on DWI may cause slow lipid diffusion and artificially reduce the measured diffusion parameters.[27] Second, many researchers believe that hepatic steatosis increases the size of hepatocytes and reduces the extracellular space, thereby reducing the ADC.[9]

Interestingly, after correcting for the effects of steatosis, we observed a stronger negative correlation between the ADC_{PDFF} and fibrosis grade than that for the ADC_u. The AUC of the ADC_{PDFF} was larger than that of the ADC_u in the classification of significant fibrosis and cirrhosis, suggesting that the ADC after correction for the effects of steatosis has greater performance in the detection of hepatic fibrosis, which might be partly explained by the greater effect of steatosis on the ADC in the early stage of liver fibrosis, as shown in our results and previous studies.[28] Imajo et al.[28] found a significant negative correlation between the PDFF and fibrosis stage, and the prevalence of steatosis was significantly higher among CHB patients with fibrosis stage ≤1,[29] suggesting that with increasing fibrosis stage, the effect of steatosis on the ADC decreases. In our study, we calculated the ADC_{PDFF} by adding 8.865× PDFF, and the added values decreased with increasing fibrosis stage, which might increase the ADC_{PDFF} differences between fibrosis grades and explain the increased correlation between the ADC_{PDFF} and fibrosis grade. Shin et al.[30] normalized the liver ADC by dividing it by the spleen ADC and found that the AUC values for the normalized liver ADC (0.777-0.875) were higher than those for the unnormalized liver ADC for each stage of fibrosis. However, the spleen ADC might be affected by iron overload and portal hypertension in CHB patients. Using the spleen ADC to standardize the liver ADC may not be appropriate in CHB patients. Therefore, our study tried to explore a new method.

Our results showed that the ADC decreases with increasing R2*, which is consistent with a biopsy-proven study in which hepatic iron grades were negatively correlated with ADCs in patients with cirrhosis.[31] This result can be explained in several aspects. First, iron shortens the T2/T2* relaxation time and reduces the liver SNR of DWI, especially on EPI sequences.[32] Second, iron-induced

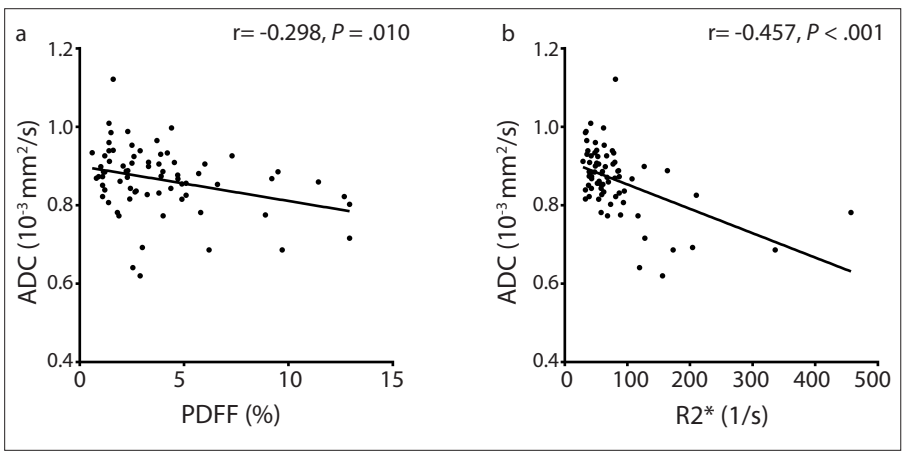

Figure 2. a, b. Correlations between ADC values and R2* and PDFF values. ADC values were negatively correlated with PDFF (r= -0.298, *P* = .010) and R2* (r= -0.457, *P* < .001) values.

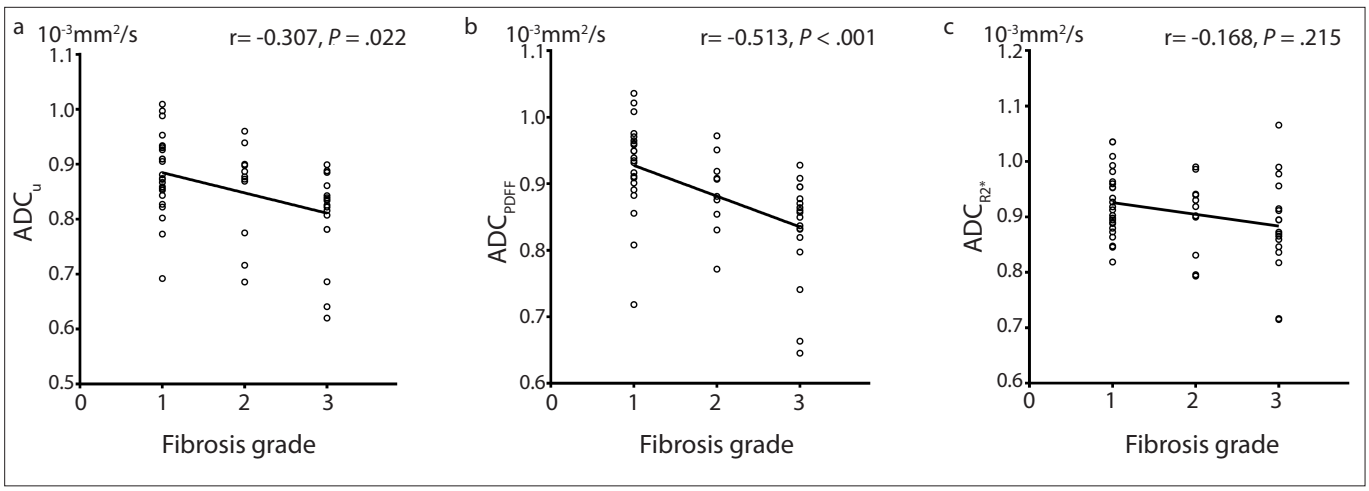

Figure 3. a–c. Comparisons of the correlation between the ADC and fibrosis grade with/without correction. The correlation of fibrosis grade with the ADC_{PDFF} was stronger than those with the ADC_u and ADC_{R2*} (r= -0.513 vs. -0.307, -0.168, respectively).

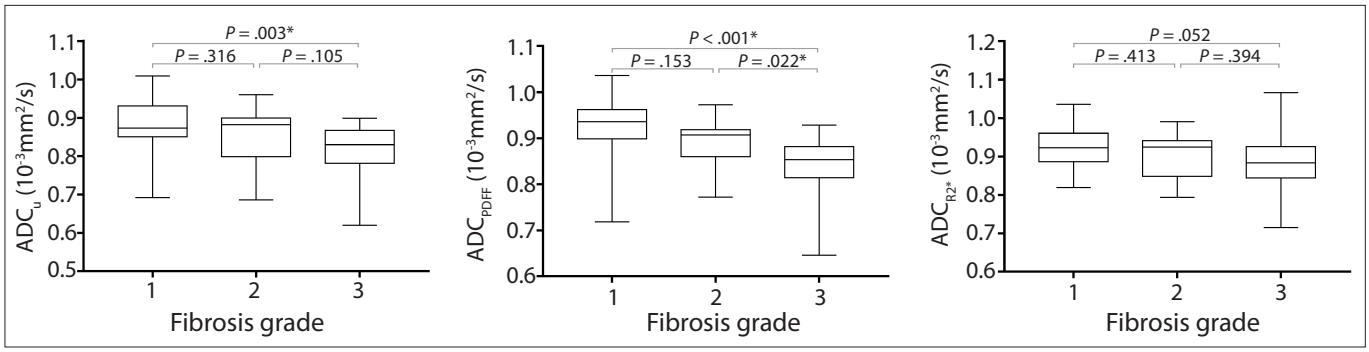

Figure 4. Box plots of the ADC_u, ADC_{PDFF}, and ADC_{R2*} according to liver fibrosis grade. The line in each box represents the median, and the horizontal boundaries of the boxes represent the first and third quartiles. The vertical error bars show the minimum and maximum values (range). After correcting for the effects of steatosis, the difference in ADC values between groups was more pronounced.

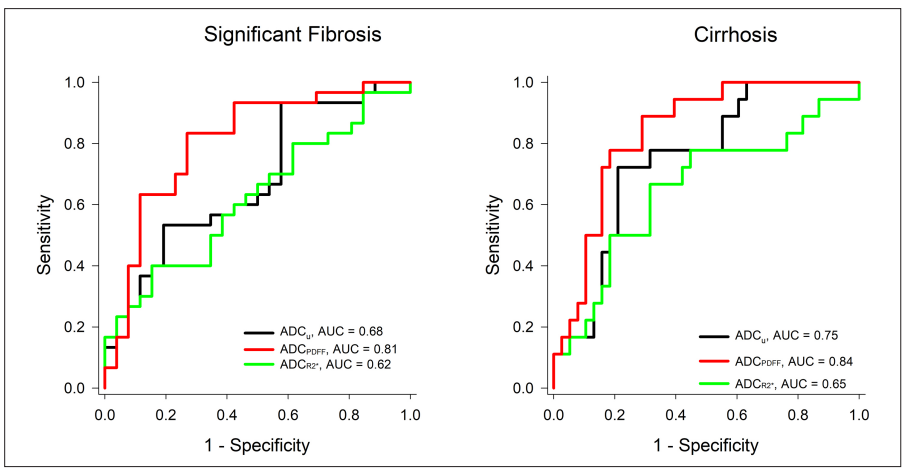

Figure 5. Receiver operating characteristic curves of the ADC_u, ADC_{PDFF}, and ADC_{R2*} in the diagnosis of significant fibrosis and cirrhosis. The AUC for the ADC_{PDFF} was significantly larger than that for the ADC_u in the diagnosis of significant fibrosis and cirrhosis.

field gradients reduce ADC values.[33] In our study, after correcting for the effects of iron, the effectiveness of the ADC in diagnosing liver fibrosis decreased. The differences in the ADC_{R2*} between fibrosis grades were reduced, possibly because R2* was positively correlated with the stage of liver fibrosis[20] and would enhance the performance of the ADC in diagnosing liver fibrosis, as some previous studies have shown.[6]

Our study has several limitations. First, liver biopsies were not performed in this study. The prevalence of steatosis is significantly higher among CHB patients with early-stage fibrosis.[29] An invasive biopsy is potentially risky due to associated complications[1] and is not readily accepted by these patients. Therefore, the APRI was used in our study, which has been recommended in international guidelines for resource-limited settings.[5] Since the APRI is influenced by many factors, the use of magnetic resonance elastography instead of the APRI might achieve more reliable results in our future study. Second, since the number of patients recruited was limited, subclassifying the subjects according to different degrees of liver fat or iron overload was not feasible. Subsequent research should expand the number of subjects, and multicenter research is needed. Third, this study evaluated only the ADC based on the monoexponential model. However, the diffusion of water molecules in many tissues of the human body does not follow a Gaussian distribution because of barriers such as cell membranes and intracellular organelles. Therefore, non-Gaussian distribution models, such as the kurtosis and biexponential models, must be explored in further studies.

In conclusion, liver steatosis and iron overload are confounding factors of the ADC in patients with CHB and can reduce ADC values. After correcting for the effects of steatosis, we observed a stronger negative correlation between the ADC_{PDFF} and fibrosis grade, and the AUC of the ADC_{PDFF} for detecting significant fibrosis and cirrhosis significantly increased. Our results indicate that the ADC corrected for the effects of steatosis may be more reliable for diagnosing liver fibrosis.

Acknowledgments

We thank the participants in this study. We thank senior clinical specialist Fangqin Gao from Siemens HealthCare for her contribution to sequence optimization on Prisma 3T MR. We thank technician Liantao Hao and Shuping Chen for their excellent technical assistance.

Financial disclosure

This research was supported by the National Natural Science Foundation of China (Grant number: 81903960) and the Natural Science Foundation of Guangdong Province of China (Grant number: 2020A1515010732).

Conflict of interest disclosure

The authors declared no conflicts of interest.

References

1. Tapper EB, Lok AS. Use of liver imaging and biopsy in clinical practice. *N Engl J Med*. 2017;377:756-768. [Crossref]
2. Lemoine M, Shimakawa Y, Nayagam S, et al. The gamma-glutamyl transpeptidase to platelet ratio (GPR) predicts significant liver fibrosis and cirrhosis in patients with chronic HBV infection in West Africa. *Gut*. 2016;65:1369-1376. [Crossref]
3. Castera L. Noninvasive methods to assess liver disease in patients with hepatitis B or C. Gastroenterology. 2012;142:1293-1302.e4. [Crossref]
4. Gao YY, Zheng J, Liang P, et al. Liver fibrosis with two-dimensional US shear-wave elastography in participants with chronic hepatitis B: A prospective multicenter study. *Radiology*. 2018; 289:407-415. [Crossref]
5. World Health Organization. Guidelines for the prevention, care and treatment of persons with chronic Hepatitis B infection. 2015.
6. Feier D, Balassy C, Bastati N, Fragner R, Wrba F, Ba-Ssalamah A. The diagnostic efficacy of quantitative liver MR imaging with diffusion-weighted, SWI, and hepato-specific contrast-enhanced sequences in staging liver fibrosis--a multiparametric approach. *Eur Radiol*. 2016;26:539-546. [Crossref]

7. Fujimoto K, Tonan T, Azuma S, et al. Evaluation of the mean and entropy of apparent diffusion coefficient values in chronic hepatitis C: correlation with pathologic fibrosis stage and inflammatory activity grade. *Radiology*. 2011;258:739-748. [Crossref]
8. Leitao HS, Doblas S, Garteiser P, et al. Hepatic Fibrosis, Inflammation, and Steatosis: Influence on the MR Viscoelastic and Diffusion Parameters in Patients with Chronic Liver Disease. *Radiology*. 2017;283:98-107. [Crossref]
9. Bulow R, Mensel B, Meffert P, Hernando D, Evert M, Kuhn JP. Diffusion-weighted magnetic resonance imaging for staging liver fibrosis is less reliable in the presence of fat and iron. *Eur Radiol*. 2013;23:1281-1287. [Crossref]
10. Karlsson M, Ekstedt M, Dahlstrom N, et al. Liver R2* is affected by both iron and fat: A dual biopsy-validated study of chronic liver disease. *J Magn Reson Imaging*. 2019;50:325-333. [Crossref]
11. Dieckmeyer M, Ruschke S, Eggers H, et al. ADC Quantification of the vertebral bone marrow water component: removing the confounding effect of residual fat. *Magn Reson Med*. 2017;78:1432-1441. [Crossref]
12. Ebrahimi B, Saad A, Jiang K, et al. Renal adiposity confounds quantitative assessment of markers of renal diffusion with MRI: a proposed correction method. *Invest Radiol*. 2017;52:672-679. [Crossref]
13. Jain A, Bhayana S, Vlasschaert M, House A. A formula to predict corrected calcium in haemodialysis patients. *Nephrol Dial Transplant*. 2008;23:2884-2888. [Crossref]
14. Xiao GQ, Zhu SX, Xiao X, Yan LN, Yang JY, Wu G. Comparison of laboratory tests, ultrasound, or magnetic resonance elastography to detect fibrosis in patients with nonalcoholic fatty liver disease: A meta-analysis. *Hepatology*. 2017;66:1486-1501. [Crossref]
15. Xiao GQ, Yang JY, Yan LN. Comparison of diagnostic accuracy of aspartate aminotransferase to platelet ratio index and fibrosis-4 index for detecting liver fibrosis in adult patients with chronic hepatitis B virus infection: a systemic review and meta-analysis. *Hepatology*. 2015;61:292-302. [Crossref]
16. Bashir MR, Wolfson T, Gamst AC, et al. Hepatic R2* is more strongly associated with proton density fat fraction than histologic liver iron scores in patients with nonalcoholic fatty liver disease. *J Magn Reson Imaging*. 2019;49:1456-1466. [Crossref]
17. Hines CD, Frydrychowicz A, Hamilton G, et al. T(1) independent, T(2) (*) corrected chemical shift based fat-water separation with multi-peak fat spectral modeling is an accurate and precise measure of hepatic steatosis. *J Magn Reson Imaging*. 2011; 33:873-881. [Crossref]
18. Hetterich H, Bayerl C, Peters A, et al. Feasibility of a three-step magnetic resonance imaging approach for the assessment of hepatic steatosis in an asymptomatic study population. *Eur Radiol*. 2016;26:1895-1904. [Crossref]
19. Zhao YZ, Gan YG, Zhou JL, et al. Accuracy of multi-echo Dixon sequence in quantification of hepatic steatosis in Chinese children and adolescents. *World J Gastroenterol*. 2019;25:1513-1523. [Crossref]
20. Hu FB, Yang R, Huang ZX, et al. 3D Multi-Echo Dixon technique for simultaneous assessment of liver steatosis and iron overload in patients with chronic liver diseases: a feasibility study. *Quant Imaging Med Surg*. 2019;9:1014-1024. [Crossref]
21. Bakan AA, Inci E, Bakan S, Gokturk S, Cimilli T. Utility of diffusion-weighted imaging in the evaluation of liver fibrosis. *Eur Radiol*. 2012;22:682-687. [Crossref]
22. Sandrasegaran K, Akisik FM, Lin C, et al. Value of diffusion-weighted MRI for assessing liver fibrosis and cirrhosis. *AJR Am J Roentgenol*. 2009;193:1556-1560. [Crossref]
23. Taouli B, Tolia AJ, Losada M, et al. Diffusion-weighted MRI for quantification of liver fibrosis: preliminary experience. *AJR Am J Roentgenol*. 2007;189:799-806. [Crossref]
24. Mehta KJ, Farnaud SJ, Sharp PA. Iron and liver fibrosis: Mechanistic and clinical aspects. *World J Gastroenterol*. 2019;25:521-538. [Crossref]
25. Moris W, Verhaegh P, Jonkers D, Deursen CV, Koek G. Hyperferritinemia in nonalcoholic fatty liver disease: iron accumulation or inflammation? *Semin Liver Dis*. 2019;39:476-482. [Crossref]
26. Wagner M, Corcuera-Solano I, Lo G, et al. Technical failure of MR elastography examinations of the liver: experience from a large single-center study. *Radiology*. 2017;284:401-412. [Crossref]
27. Baron P, Dorrius MD, Kappert P, Oudkerk M, Sijens PE. Diffusion-weighted imaging of normal fibroglandular breast tissue: influence of microperfusion and fat suppression technique on the apparent diffusion coefficient. *NMR Biomed*. 2010;23:399-405. [Crossref]
28. Imajo K, Kessoku T, Honda Y, et al. Magnetic resonance imaging more accurately classifies steatosis and fibrosis in patients with nonalcoholic fatty liver disease than transient elastography. *Gastroenterology*. 2016;150:626-637.e7. [Crossref]
29. Shi JP, Fan JG, Wu R, et al. Prevalence and risk factors of hepatic steatosis and its impact on liver injury in Chinese patients with chronic hepatitis B infection. *J Gastroenterol Hepatol*. 2008;23:1419-1425. [Crossref]
30. Shin MK, Song JS, Hwang SB, Hwang HP, Kim YJ, Moon WS. Liver fibrosis assessment with diffusion-weighted imaging: value of liver apparent diffusion coefficient normalization using the spleen as a reference organ. *Diagnostics (Basel)*. 2019; 9:107. [Crossref]
31. Chandarana H, Do RK, Mussi TC, et al. The effect of liver iron deposition on hepatic apparent diffusion coefficient values in cirrhosis. *AJR Am J Roentgenol*. 2012;199:803-808. [Crossref]
32. Pierre TG, Clark PR, Chua-anusorn W, et al. Noninvasive measurement and imaging of liver iron concentrations using proton magnetic resonance. *Blood*. 2005;105:855-861. [Crossref]
33. Metens T, Ferraresi KF, Farchione A, Moreno C, Bali MA, Matos C. Normal hepatic parenchyma visibility and ADC quantification on diffusion-weighted MRI at 3 T: influence of age, gender, and iron content. *Eur Radiol*. 2014;24:3123-3133. [Crossref]